

Two-Triplet-Dimer Excitation Spectra in the Shastry-Sutherland Model for $\text{SrCu}_2(\text{BO}_3)_2$

Yoshiyuki FUKUMOTO*

Department of Physics, Faculty of Science and Technology, Science University of Tokyo, Noda, Chiba 278-8510

(Received)

By using the perturbation expansion up to the fifth order, we study the two-triplet-dimer excitation spectra in the Shastry-Sutherland model, where the localized nature of a triplet-dimer, the propagation of a triplet-dimer pair by the correlated hopping and the long-range interactions between triplet-dimers play an essential role. It is found that the dispersion relations for first-neighbor triplet-dimer pair excitations with $S = 1$ and p -type symmetry qualitatively explain the second-lowest branch observed in the neutron inelastic scattering experiment. It is also predicted that the second-lowest branch consists of two components, p_x - and p_y -states, with slightly different excitation energies. The origin of the singlet mode at 3.7meV observed in the Raman scattering experiment is also discussed.

KEYWORDS: $\text{SrCu}_2(\text{BO}_3)_2$, Shastry-Sutherland model, two dimensions, bound state, Heisenberg antiferromagnet, perturbation expansion, dispersion relation

There has been a growing interest in low-dimensional quantum spin systems, since one can observe a variety of properties where classical pictures break down. In the last decade, spin gapped ground states, particularly, in two-dimensional systems have received considerable attention in connection with the high- T_c superconductivity. For instance, a quasi-two-dimensional compound CaV_4O_9 is known to have a spin gap originating in the plaquette RVB mechanism.^{1, 2, 3, 4)}

Two years ago, another new two-dimensional spin gap system $\text{SrCu}_2(\text{BO}_3)_2$ was found by Kageyama *et al.*⁵⁾ In this compound, magnetic ions Cu^{2+} ($S = 1/2$) are arranged as shown in Fig. 1. Miyahara and Ueda⁶⁾ pointed out that $\text{SrCu}_2(\text{BO}_3)_2$ is an experimental realization of a special class of the Heisenberg antiferromagnets which is called the Shastry-Sutherland model⁷⁾

$$\mathcal{H} = \sum_{\langle i, j \rangle} \mathbf{S}_i \cdot \mathbf{S}_j + \lambda \sum_{\langle\langle i, j \rangle\rangle} \mathbf{S}_i \cdot \mathbf{S}_j, \quad (1)$$

where $\langle i, j \rangle$ ($\langle\langle i, j \rangle\rangle$) denotes a (next-)nearest-neighbor pair of spins. The strength of the interdimer coupling is now considered $\lambda \sim 0.63$.^{8, 9)} The orthogonal dimer structure as seen in Fig. 1 leads to the following unique properties: the direct product of the singlet-dimer states of the nearest-neighbor pairs of spins is the ground state exactly for $\lambda < \sim 0.7$ and a triplet-dimer in the singlet sea is almost localized.^{6, 9)}

The nature of the quantum phase transition has been one of important subjects in theoretical investigations.^{6, 9, 10, 11, 12)} At first stage of the investigations, it was assumed that the exact dimer singlet state is destabi-

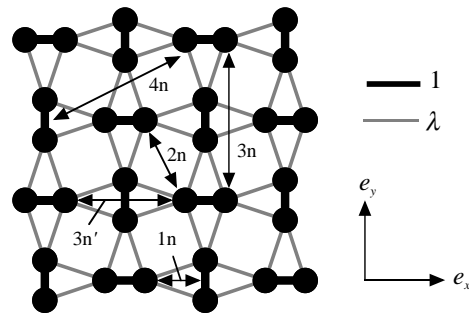


Fig. 1. Structure of a two-dimensional network formed by Cu^{2+} in $\text{SrCu}_2(\text{BO}_3)_2$. The closed circles represent copper ions. The nearest-neighbor bonds are expressed by the bold lines and the next nearest-neighbor bonds by the gray lines. The vectors, \mathbf{e}_x and \mathbf{e}_y , are the primitive translation vectors in this lattice. Note that there exist two types of third-neighbor triplet-dimer pairs, which are indicated by $3n$ and $3n'$. For brevity, we call the former the third-neighbor pair. Within the fifth-order calculation, the diagonal interactions between triplet-dimers appear for the first-neighbor ($1n$), second-neighbor ($2n$), third-neighbor ($3n$) and fourth-neighbor ($4n$) triplet-dimer pairs.

lized against the Néel ordered state when λ is increased. A recent study, however, suggested that there exists an intermediate phase, where a plaquette RVB state is stabilized, between the exact dimer singlet phase and the Néel ordered phase.¹²⁾ The first-order transition point between the exact dimer singlet phase and the plaquette RVB phase was estimated as $\lambda_c = 0.677$ by using the series expansion method. Another interesting topics in $\text{SrCu}_2(\text{BO}_3)_2$ is that the magnetization plateaus are observed at $1/3$, $1/4$ and $1/8$ of the full Cu moment.^{5, 13)} The localized nature of a triplet-dimer plays an impor-

* E-mail: yfuku@ph.noda.sut.ac.jp

tant role in the appearance of the plateaus.^{6,14,15,16)}

As mentioned above, a triplet-dimer is hard to propagate in the singlet sea because of the orthogonal dimer structure. In precise, the orthogonal dimer structure prohibits the propagation of a triplet-dimer up to the fifth-order perturbation in λ .^{6,15)} Recently, almost flat band of the single-triplet-dimer excitations at 3.0meV was observed in the neutron inelastic scattering experiment by Kageyama *et al.*¹⁷⁾

In this neutron inelastic scattering experiment, multiple-triplet-dimer excitation spectra were also observed, which show rather dispersive behavior compared with the single-triplet-dimer excitation. In the ESR measurement, the second spin-gap was observed at 4.7meV, which corresponds to the band bottom of the second-lowest spectrum.¹⁸⁾ Note that the localized nature of a triplet-dimer leads to almost flat bands of multiple-triplet-dimer continua and makes the experimental observation of various multiple-triplet-dimer bound states possible. The observation of a singlet bound state at 3.7meV in the Raman scattering experiment has been also reported.¹⁹⁾

In this letter, we study the two-triplet-dimer excitations by the fifth-order perturbation expansion. We here mention the relation between the present problem and the two-magnon bound state in the Ising-Heisenberg ferromagnets which is now well understood.²⁰⁾ In the Ising-Heisenberg model, when the hopping of a magnon is suppressed by the Ising-like exchange anisotropy, the formation of the two-magnon bound states is more favored and the band of those states becomes more narrow. Within the first-order perturbation, the mechanism of the formation of two-triplet-dimer bound states in the present model is the same as that of the two-magnon bound states in the Ising limit of the Ising-Heisenberg model.

In the Shastry-Sutherland model, the two-triplet-dimer bound state problem becomes to be more interesting due to the following two reasons arising from higher-order perturbation processes. First, the range of the diagonal interactions between triplet-dimers is enlarged when the order of the perturbation is extended. Second, the correlated hopping, where a triplet dimer can hop when the rest spectator triplet-dimer always lies at a neighboring site before and after the hopping, is possible in the lower-order perturbation processes than the six order which leads to the single-triplet-dimer hopping.^{14,15,16)} The former separates a branch of two-triplet-dimer bound states from the two-triplet-dimer continuum. The latter make such the branch a dispersive one. It is also important to observe these higher-order effects pronouncedly that SrCu₂(BO₃)₂ locates near the first-order transition point. We expect that the two facts mentioned above and the localized nature of a triplet-dimer are properly taken into account in our fifth-order perturbation calculation.

We now turn to the calculation of matrix elements in the fifth-order effective Hamiltonian, H^{eff} , for the subspace composed of two triplet-dimers. We write the two-

triplet-dimer states as

$$|\mathbf{r}, \boldsymbol{\delta}, S\rangle \equiv \sum_{m=-1}^1 C(S, m) |t_m\rangle_{\mathbf{r}} |t_{-m}\rangle_{\mathbf{r}+\boldsymbol{\delta}} \prod'_{\mathbf{r}'} |s\rangle_{\mathbf{r}'}, \quad (2)$$

where $S = 0, 1, 2$. In this definition, $|s\rangle_{\mathbf{r}}$ represents the singlet state of the dimer at \mathbf{r} , and $|t_m\rangle_{\mathbf{r}}$ represents the triplet state with the total S^z of m . The prime attached on the product symbol means the exception of the sites \mathbf{r} and $\mathbf{r} + \boldsymbol{\delta}$. The explicit expression of $C(S, m)$ is given by

$$C = \begin{bmatrix} -1/\sqrt{3} & 1/\sqrt{3} & -1/\sqrt{3} \\ 1/\sqrt{2} & 0 & -1/\sqrt{2} \\ 1/\sqrt{6} & 2/\sqrt{6} & 1/\sqrt{6} \end{bmatrix}, \quad (3)$$

where the row (column) index runs $S = 0, 1, 2$ ($m = -1, 0, 1$). Note that there is a symmetry relation $C(S, -m) = (-1)^S C(S, m)$. The relative vector between the two triplet-dimers, $\boldsymbol{\delta}$, is assumed to satisfy $\delta_x > 0$ or $\delta_x = 0, \delta_y > 0$ in the practical calculations.

The interactions between two triplet-dimers within fifth-order approximation are given by

$$V_{\mathbf{r}, \boldsymbol{\delta}}(S) = \langle \mathbf{r}, \boldsymbol{\delta}, S | H^{\text{eff}} | \mathbf{r}, \boldsymbol{\delta}, S \rangle - (E_g + 2\Delta_{\text{sg}}), \quad (4)$$

where $E_g = -3N_{\text{D}}/4$ is the ground state energy of the system with N_{D} dimers and

$$\Delta_{\text{sg}} = 1 - \lambda^2 - \frac{\lambda^3}{2} - \frac{\lambda^4}{8} + \frac{5\lambda^5}{32} \quad (5)$$

is the fifth-order series of the spin gap.^{6,9)} Nonzero elements of $V_{\mathbf{r}, \boldsymbol{\delta}}(S)$ are summarized in Table I. The interactions for $S = 2$ have been calculated already up to the third order and the first-order repulsion between the first-neighbor triplet-dimers is known to lead to the 1/2-plateau.^{14,15,16)} On the other hand, we find in Table I that the first-order interactions between first-neighbor triplet-dimers for $S = 0$ and 1 are attractive.

Table I. Nonzero elements of the diagonal interactions between two triplet-dimers, $V_{\mathbf{r}, \boldsymbol{\delta}}(S)$. A set of $(\mathbf{r}, \boldsymbol{\delta})$ for first-, second-, third- or fourth-neighbor triplet-dimer pairs is, respectively, denoted by 1n, 2n, 3n or 4n. (See Fig. 1.)

$(\mathbf{r}, \boldsymbol{\delta})$	S	$V_{\mathbf{r}, \boldsymbol{\delta}}(S)$
1n	0	$\lambda(-16 + 8\lambda + 16\lambda^2 + 18\lambda^3 - \lambda^4)/16$
	1	$\lambda(-8 + 16\lambda + 14\lambda^2 - 9\lambda^3 - 16\lambda^4)/16$
	2	$\lambda(8 + 8\lambda - 2\lambda^2 - 9\lambda^3 - \lambda^4)/16$
2n	0	$\lambda^3(-16 + 45\lambda^2)/32$
	1	$\lambda^3(-4 - 6\lambda + 3\lambda^2)/16$
	2	$\lambda^3(2 + 3\lambda + 3\lambda^2)/8$
3n	0	$\lambda^2(-32 - 48\lambda + 56\lambda^2 + 289\lambda^3)/32$
	1	$\lambda^2(-32 - 48\lambda + 8\lambda^2 + 129\lambda^3)/64$
	2	$\lambda^2(32 + 48\lambda + 8\lambda^2 + 129\lambda^3)/64$
4n	0	$\lambda^4(-8 - 17\lambda)/32$
	1	$\lambda^4(-8 - 17\lambda)/64$
	2	$\lambda^4(8 + 17\lambda)/64$

We introduce the Fourier transformation of eq. (2):

$$|\mathbf{q}, \boldsymbol{\delta}, S, \alpha\rangle = \sqrt{\frac{2}{N_D}} \sum_{\mathbf{r}_\alpha} e^{i\mathbf{q}\cdot\mathbf{r}_\alpha} |\mathbf{r}_\alpha, \boldsymbol{\delta}, S\rangle, \quad (6)$$

where $\alpha (= A, B)$ denotes the sublattice index and \mathbf{r}_α denotes a site on the sublattice α . The representation of H^{eff} using this basis set becomes to be a direct sum of finite-size matrices because of the prohibition of the single-triplet-dimer hopping. In the fifth-order approximation, the representation of H^{eff} has off-diagonal matrix elements among first-, second-, fourth-neighbor triplet-dimer pair states. For the third-neighbor triplet-dimer pairs, H^{eff} has only a diagonal element, which is different from $E_g + 2\Delta_{\text{sg}}$. For the other states, H^{eff} has only the diagonal element of $E_g + 2\Delta_{\text{sg}}$.

We here mention the zeroth-order wave-functions for the first-neighbor triplet-dimer pair excitations, which are relevant to the observed multiple-triplet-dimer excitations in the neutron inelastic scattering experiment as described below. The first-order perturbation removes the degeneracy between the first-neighbor triplet-dimer pair states and the other states. We write the eigenfunctions of the eigenvalue problem to determine the second-order energies as follows:

$$|s_\xi\rangle_{S,\mathbf{q}} \equiv \frac{e^{-iq\xi}}{\sqrt{2}} |\mathbf{q}, e_\xi, S, \alpha_\xi\rangle + \frac{(-1)^S}{\sqrt{2}} |\mathbf{q}, e_\xi, S, \bar{\alpha}_\xi\rangle, \quad (7a)$$

$$|p_\xi\rangle_{S,\mathbf{q}} \equiv \frac{e^{-iq\xi}}{\sqrt{2}} |\mathbf{q}, e_\xi, S, \alpha_\xi\rangle - \frac{(-1)^S}{\sqrt{2}} |\mathbf{q}, e_\xi, S, \bar{\alpha}_\xi\rangle \quad (7b)$$

for $\xi = x, y$, where we have defined $\alpha_x \equiv A$, $\alpha_y \equiv B$, $\bar{\alpha}_x \equiv B$ and $\bar{\alpha}_y \equiv A$. Note that $|s_\xi\rangle_{S,0}$ and $|p_\xi\rangle_{S,0}$ have, respectively, the s -type and p_ξ -type symmetries. The degeneracy between the s -wave states and the p -wave states is removed by the second-order perturbation. The fourth-order perturbation removes the remaining two-fold degeneracy for each of the s -wave states and the p -wave states at the general points in the first Brillouin zone. Then the way of mixing between the two s -wave functions is determined as follows:

$$|s_+\rangle_{S,\mathbf{q}} \equiv f(q_x, q_y) |s_x\rangle_{S,\mathbf{q}} + (-1)^S f(q_y, q_x) |s_y\rangle_{S,\mathbf{q}}, \quad (8a)$$

$$|s_-\rangle_{S,\mathbf{q}} \equiv f(q_y, q_x) |s_x\rangle_{S,\mathbf{q}} - (-1)^S f(q_x, q_y) |s_y\rangle_{S,\mathbf{q}}, \quad (8b)$$

where

$$[f(q_x, q_y)]^{-2} = 1 + \left[\cos q_x - \cos q_y - \sqrt{1 + (\cos q_x - \cos q_y)^2} \right]^2. \quad (9)$$

The results of the fifth-order perturbation expansion of excitation energies, ΔE , for all the two-triplet-dimer excitations are shown in Fig. 2, where we choose $\lambda = 0.55$. In this figure, the results except for the second- and fourth-neighbor triplet-dimer pairs are obtained by the usual series expansion. For the second- and fourth-

neighbor triplet-dimer pairs, the mixing among these states at high-symmetry points of \mathbf{q} occurs in the fifth order, which makes the convergence of the series slow around such the high-symmetry points. To avoid this, we diagonalize directly the effective Hamiltonian for the subspace of the second- and fourth-neighbor triplet-dimer pair states, which is an hermitian matrix obtained by making further partial diagonalization for H^{eff} . The resultant eigenvalues are plotted in Fig. 2 as the solid lines. Roughly speaking, almost dispersionless bands indicated by "4n" originate in the fourth-neighbor triplet-dimer pairs. The other solid lines originate in the second-neighbor triplet-dimer pairs.

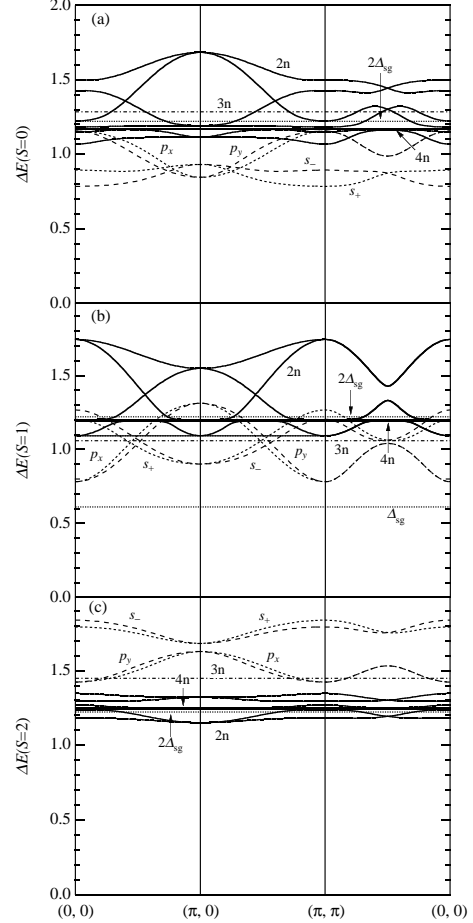


Fig. 2. Dispersion relations of the two-triplet-dimer states for (a) $S = 0$, (b) $S = 1$ and (c) $S = 2$, where we choose $\lambda = 0.55$. For $S = 1$, dispersion relation of the single-triplet-dimer states is also shown.

We find dispersive behavior for the branches of the first-neighbor triplet-dimer pairs for $S = 0, 1$ and 2 , which can propagate in the singlet sea from the third order. It should be stressed that the dispersion relation of the first-neighbor triplet-dimer pairs with p -type symmetry for $S = 1$ qualitatively explains the behavior of the second-lowest branch in the neutron scattering experiment. (See Fig. 3 in Ref. 17.) Very recently, a neutron

inelastic scattering experiment under the magnetic fields was carried out.²¹⁾ This experiment revealed that the total spin of the second-lowest branch is one, which is also consistent with our result. Note that the fourth-order terms remove the two-fold degeneracy between p_x - and p_y -type first-neighbor two-triplet-dimer pairs at general points in the first Brillouin zone. The explicit expressions of the excitation energies are given by

$$\begin{aligned} \Delta E_{p_x}(S=1) = & 2 - \frac{\lambda}{2} - \frac{3\lambda^2}{4} - \frac{\lambda^3}{4}(1 + \cos q_x \cos q_y) \\ & - \frac{\lambda^4}{16}(35 + 15 \cos q_x \cos q_y - 2 \cos^2 q_y \sin^2 q_x) \\ & - \frac{\lambda^5}{64}[274 + 175 \cos q_x \cos q_y - 8 \cos^2 q_x \\ & \times \{1 + (6 + \cos q_x \cos q_y) \sin^2 q_y\}], \quad (10a) \end{aligned}$$

$$\Delta E_{p_y}(S=1) = (q_x \leftrightarrow q_y \text{ in rhs of eq. (10a)}), \quad (10b)$$

for the p_x - and p_y -states, respectively. As seen in the above equations and Fig. 2(b), the observed second-lowest branch is composed of two components with slightly different energies on the path from the Γ point to the X point and on the path from the X point to the M point, which may be detected by careful analysis of the experimental data.

We turn to the second-neighbor triplet-dimer pairs. From Fig. 2, we find dispersive behavior for $S=0$ and 1, but we find rather flat bands for $S=2$. Note that the effective Hamiltonian for $S=2$ is nothing but the two-body part in the subspace of the effective Hamiltonian dominating the magnetization process. Rather small energy-gain by the correlated hopping for $S=2$ seems to be consistent with the appearance of the magnetization plateaus in $\text{SrCu}_2(\text{BO}_3)_2$. In Ref. 16, where the magnetization plateaus are studied by the third-order perturbation, it was assumed that the states with first-neighbor triplet-dimer pairs can be truncated. We find in Fig. 2(c) that the excitation energies of the first-neighbor two-triplet-dimer pairs for $S=2$ are not the lowest lying branch even when the fourth- and fifth-order terms are taken into account. This finding gives a support to the treatment in Ref. 16.

As for the third-neighbor triplet-dimer pairs, the binding energies are not so small, but propagation does not occur within the fifth-order perturbation. The fourth-neighbor triplet-dimer pairs can propagate from the fifth order but the band width is too narrow to see in this figure.

In Fig. 3, we show the minimum two-triplet-dimer excitation energies as a function of λ . For $S=1$, the result of the exact diagonalization on a finite-size cluster with $N_D=10$ is also shown. We find that the series of the two-triplet-dimer excitation for $S=0$ and $S=2$ tends to converge within the present calculation. In particular, the fifth-order perturbation series results in 3.7meV for the minimum energy of the singlet two-triplet-dimer excitation for $\text{SrCu}_2(\text{BO}_3)_2$ with $\lambda=0.63$ and the in-

tradimer exchange constant of 7.3meV. This value agrees with the observed singlet excitation energy in the Raman scattering experiment.¹⁹⁾ As for $S=1$, the result in Fig. 3(b) indicates that we should extend the order of perturbation to obtain the quantitative description of $\text{SrCu}_2(\text{BO}_3)_2$. Note that the exact diagonalization gives 4.6meV for the minimum two-triplet-dimer excitation energy for $\text{SrCu}_2(\text{BO}_3)_2$, which agrees with the results of the neutron inelastic scattering experiment¹⁷⁾ and the ESR measurement.¹⁸⁾ Our fifth-order result of this excitation energy is lower than that of the exact diagonalization. If higher-order terms beyond the fifth order are taken into account, then the binding energy is expected to be suppressed due to the single-triplet-dimer hopping.

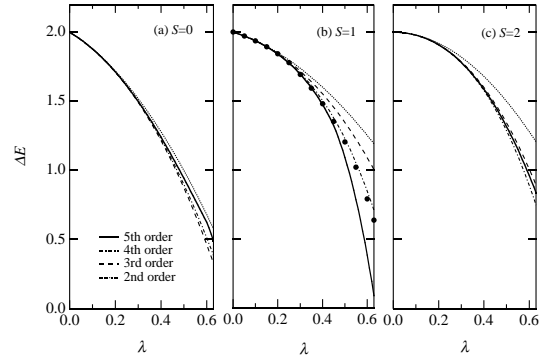


Fig. 3. The minimum two-triplet-dimer excitation energies as a function of λ for (a) $S=0$, (b) $S=1$ and (c) $S=2$. The solid, dash-dotted, long-dashed and short-dashed lines, respectively, represent the fifth-, fourth-, third- and second-order results. The closed circles in (b) are the results of the exact diagonalization for the finite-size cluster with $N_D=10$.

In summary, we have studied the two-triplet-dimer excitations in the Shastry-Sutherland model by using the fifth-order perturbation. It has been found that the second-lowest branch observed in the neutron scattering experiment and the singlet state at 3.7meV observed in the Raman scattering experiment originate from the first-neighbor two-triplet-dimer excitations. It has been also pointed out that the second-lowest branch in the neutron scattering experiment is composed of two components, p_x - and p_y -states, whose degeneracy is removed by the fourth-order perturbation. We expect that such the structure is confirmed by the careful analysis of the experimental data.

The author would like to thank Prof. A. Oguchi for useful discussions and critical reading of the manuscript. We have used a part of the codes provided by H. Nishimori in TITPACK Ver. 2.

-
- [1] S. Taniguchi, T. Nishikawa, Y. Yasui, Y. Kobayashi, M. Sato, T. Nishioka, M. Kontani and K. Sano: J. Phys. Soc. Jpn. **64** (1995) 2758.
 - [2] K. Kodama, H. Harashina, H. Sasaki, Y. Kobayashi, M. Kasai, S. Taniguchi, Y. Yasui, M. Sato, K. Kakurai, T. Mori and M. Nishi: J. Phys. Soc. Jpn. **66** (1997) 793.

- [3] K. Ueda, H. Kontani, M. Sigrist and P. A. Lee: Phys. Rev. Lett. **76** (1996) 1932.
- [4] Y. Fukumoto and A. Oguchi: J. Phys. Soc. Jpn. **67** (1998) 2205.
- [5] H. Kageyama, K. Yoshimura, R. Stern, N. V. Mushnikov, K. Onizuka, M. Kato, K. Kosuge, C. P. Slichter, T. Goto and Y. Ueda: Phys. Rev. Lett. **82** (1999) 3168.
- [6] S. Miyahara and K. Ueda: Phys. Rev. Lett. **82** (1999) 3701.
- [7] S. Shastry and B. Sutherland: Physica **108B** (1981) 1069.
- [8] S. Miyahara and K. Ueda: preprint.
- [9] Z. Weihong, C. J. Hamer and J. Oitmaa: Phys. Rev. **B60** (1999) 6608.
- [10] M. Albrecht and F. Mila: Europhys. Lett. **34** (1996) 145.
- [11] E. Muller-Hartmann, R. R. P. Singh, C. Knetter and G. S. Uhrig: cond-mat/9910165.
- [12] A. Koga and N. Kawakami: preprint.
- [13] H. Kageyama, Y. Narumi, K. Kindo, K. Onizuka, Y. Ueda and T. Goto: preprint.
- [14] T. Momoi and K. Totsuka: Phys. Rev. **B61** (2000) 3231.
- [15] S. Miyahara and K. Ueda: Phys. Rev. **B61** (2000) 3417.
- [16] Y. Fukumoto and A. Oguchi: J. Phys. Soc. Jpn. (in press.)
- [17] H. Kageyama, M. Nishi, N. Aso, K. Onizuka, T. Yoshimura, K. Nukui, K. Kodama, K. Kakurai and Y. Ueda: preprint.
- [18] H. Nojiri, H. Kageyama, K. Onizuka, Y. Ueda and M. Motokawa: J. Phys. Soc. Jpn. **68** (1999) 2906.
- [19] P. Lemmens, M. Grove, M. Fischer, G. Guntherodt, V. N. Kotov, H. Kageyama, K. Onizuka and Y. Ueda: cond-mat/0003094.
- [20] I. Ono, S. Mikado and T. Oguchi: J. Phys. Soc. Jpn. **30** (1971) 358.
- [21] K. Kakurai: private communication.